European Journal of Medicinal Chemistry 101 (2015) 52–62

Contents lists available at ScienceDirect

European Journal of Medicinal Chemistry

journal homepage: http://www.elsevier.com/locate/ejmech

Research paper

Synthesis, antiplasmodial activity and mechanistic studies of pyrimidine-5-carbonitrile and quinoline hybrids

Hardeep Kaur [a], Jan Balzarini [b], Carmen de Kock [c], Peter J. Smith [c], Kelly Chibale [d], Kamaljit Singh [a, *]

[a] Department of Chemistry, UGC-Centre of Advance Study-II, Guru Nanak Dev University, Amritsar 143005, India
[b] Rega Institute for Medical Research, KU Leuven, 10 Minderbroedersstraat, B-3000 Leuven, Belgium
[c] Division of Pharmacology, Department of Medicine, University of Cape Town, Observatory 7925, South Africa
[d] Department of Chemistry, South African Medical Research Council Drug Discovery and Development Research Unit, Institute of Infectious Disease and Molecular Medicine, University of Cape Town, Rondebosch 7701, South Africa

ARTICLE INFO

Article history:
Received 14 November 2014
Received in revised form
19 May 2015
Accepted 8 June 2015
Available online 12 June 2015

Keywords:
Antiplasmodial agents
4-Aminoquinoline
Heme binding
Cytotoxic activity
Pyrimidine
Hybrid antimalarials

ABSTRACT

A series of hybrids comprising of 5-cyanopyrimidine and quinoline moiety were synthesized and tested for *in vitro* antiplasmodial activity against NF54 and Dd2 strains of *Plasmodium falciparum*. Hybrid bearing *m*-nitrophenyl substituent at C-4 of pyrimidine displayed the highest antiplasmodial activity [IC_{50} = 56 nM] against the CQ^R (Dd2) strain, which is four–fold greater than CQ.

1. Introduction

Malaria is one of the major causes of morbidity and mortality around the globe and is caused by protozoa of the genus *Plasmodium* of which *Plasmodium falciparum* is the most lethal and widespread species. Recent report of the WHO [1] indicated over 190 million cases of malaria and approximately 5,84,000 deaths in 2013. The emerging resistance to the existing antiplasmodial drugs [2], absence of new antiplasmodial drugs [3] and the slow pace of the development of clinically approved vaccines [4] further compromise the efficient control of this disease. With no licensed malaria vaccines currently in hand, several vaccine projects are in clinical trials, and of these, the most advanced vaccine (RTS, S/AS01) has been evaluated in a Phase 3 clinical trial and is active only against *P. falciparum*. The situation is further exacerbated by the decreased clinical efficacy of front-line artemisinin combination therapies (ACTs) currently used for the treatment of malaria [5]. These factors exemplify the need to discover new, effective, and affordable antiplasmodial chemotherapeutic agents acting through novel mechanisms.

Substituted quinolines are historically [6] among the most important antiplasmodial agents and their vast use in the 20th century provided well founded hopes for the eradication of malaria. The most important drugs of this family include chloroquine (CQ, **1**), quinine, mefloquine, amodiaquine, piperaquine and primaquine (Fig. 1). CQ and related 4-aminoquinolines are believed to inhibit the formation of crystalline hemozoin from free ferriprotoporphyrin IX, which is generated during proteolysis of host hemoglobin in the acidic food vacuole (FV) and is toxic to the parasite [6,7]. However, the extensive use of CQ for the treatment of *P. falciparum* malaria led to the development of resistance, which is linked to the mutations in the FV membrane protein *Pf*crt (*P. falciparum* chloroquine resistance transporter), which might result in reduced accumulation of CQ in chloroquine-resistant strains [8,9].

To overcome CQ-resistance by *P. falciparum*, the hybridization approach has proven to be a promising tool as the hybrid drugs act through different mechanisms against either a single or multiple targets and lead to acceptable pharmacological and safety profiles

* Corresponding author.
E-mail address: kamaljit.chem@gndu.ac.in (K. Singh).

http://dx.doi.org/10.1016/j.ejmech.2015.06.024
0223-5234/

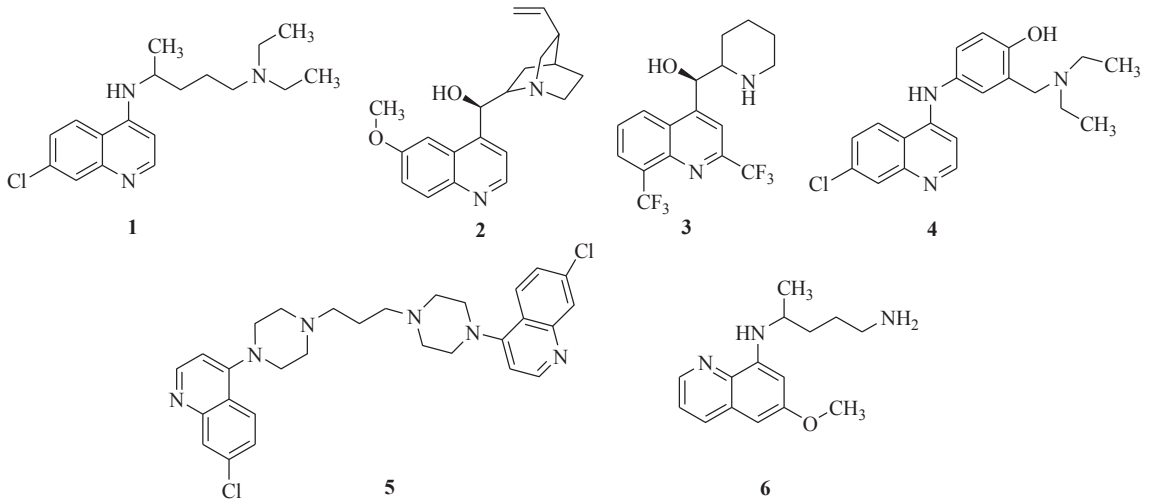

Fig. 1. Quinoline based antimalarial drugs.

[10]. In the design of hybrid drugs, the 4-aminoquinoline nucleus has received increasing attention owing to their low cost and good activity–toxicity profiles. Pyrimidines being one of the essential cell constituents represent one of the most important heterocycles that exhibit remarkable pharmacological activities [11]. Pyrimidines bearing a nitrile war head were reported to display excellent inhibitory activity against both falcipain-2 as well as cultured *P. falciparum.* [12]. The nitrile groups are known to exert antiplasmodial effect by forming a reversible thioimidate intermediate with cysteine residues of cysteine proteases, which ultimately results in the inhibition of the enzyme [13–15].

In our previous reports on pyrimidine-quinoline hybrids [16], we demonstrated high (nM) antiplasmodial activity of this class of hybrids against both chloroquine-sensitive (CQ^S) and chloroquine-resistant (CQ^R) strains of *P. falciparum*, which in some cases was even greater than CQ. As an extension of our research interest in this class of hybrids, we herein report on the synthesis and antiplasmodial activity of novel pyrimidine-quinoline hybrids bearing a cyano group at the C-5 position of the pyrimidine, which is covalently linked to the quinoline ring through different linkers. Further, we also report on the efficacy of these hybrids to bind heme as well as μ-oxo heme in order to understand the possible mode of action of these hybrids.

2. Chemistry

Pyrimidine-quinoline hybrids reported in this work were prepared using the synthetic protocol outlined in Scheme 1. The substituted pyrimidin-6(1*H*)-ones **10** were prepared by using a modified Biginelli condensation reaction of ethyl cyanoacetate **7**, appropriately substituted benzaldehyde **8** and S-methylisothiourea hemisulphate salt **9a**/N-morpholinyl guanidine hydrochloride **9b**, in ethanol in the presence of K_2CO_3 [17]. Further, treatment of appropriate **10** with excess $POCl_3$ afforded the corresponding 6-chloropyrimidine derivatives **11**, in quantitative yields. The nucleophilic displacement reaction of **11** with 7-chloro-4-aminoquinoline [18] **12** in dry THF yielded corresponding hybrids **13** in 82–92% (Table 1) after column chromatographic purification. The structures of all the hybrids were established on the basis of spectral (^{1}H NMR, ^{13}C NMR, EIMS, FTIR) as well as microanalytical data (*vide experimental*). The structure of **13d** was additionally confirmed by single crystal x-ray analysis (Table S1). The ortep diagram of **13d** is shown in Fig. 2.

3. Results and discussion

3.1. In vitro antiplasmodial activity and structure–activity relationships (SARs)

The hybrids **13a**–**l** were evaluated for their activity against CQ^S (NF 54) and CQ^R (Dd2) strains of *P. falciparum* using CQ and artesunate (ASN) reference drugs. The concentrations inhibiting 50% of parasite growth (IC_{50}) were obtained using a non-linear dose–response curve fitting analysis *via* Graph Pad Prism v.4.0 software (Table 1). Analysis of the antiplasmodial activity data revealed that most of the hybrids (except **13d** and **13g**) showed significant (nM) activity against CQ^S [43.8–197.9 nM (NF54)] as well as CQ^R strains [55.8–1529.7 nM (Dd2)] of *P. falciparum*. Among all the hybrids assayed, hybrid **13e** depicted the highest antiplasmodial activity [IC_{50} = 55.8 nM (Dd2)] against the CQ^R strain, which is four–fold greater than CQ [IC_{50} = 257.6 nM (Dd2)]. Comparison of antiplasmodial activity of the homologues **13a** [IC_{50} = 133.7 nM (NF54); 319.4 nM (Dd2)] and **13b** [IC_{50} = 108.6 nM (NF54); 295.2 nM (Dd2)] showed that a four-methylene spacer confers superior antiplasmodial activity compared to a three-methylene spacer. Further, the replacement of the flexible aliphatic linker of **13a–c** with a piperazinyl linker in **13d**, led to a complete loss of activity. It is possibly due to the steric restrictions conferred by the piperazinyl linker (Fig. 2b) in **13d**, which may restrict face-to-face stacking of the quinoline unit with heme [19], leading to inefficient inhibition of the heme polymerization to hemozoin. This fact is experimentally supported by titration of monomeric heme with **13d**. Gradual addition of 0–37.3 μM of **13d** (Figs. S1–S2) to a solution of monomeric heme (2.4 μM, DMSO:H_2O/4:6, v/v) revealed no change in the absorbance at 402 nm indicating lack of a binding interaction.

Similarly, replacement of the diaminopropyl linker with a less basic aminopropoxy linker in **13c** caused a marginal increase in the antiplasmodial activity against both the tested *P. falciparum* strains. This is in contrast to our earlier finding [16c], where a similar change of the linker led to significant loss in antiplasmodial activity. However, in addition to the nature of the linker, the antiplasmodial activity of the current series of pyrimidine-quinoline hybrids seems to be benefitted by the presence of a cyano group on the pyrimidine

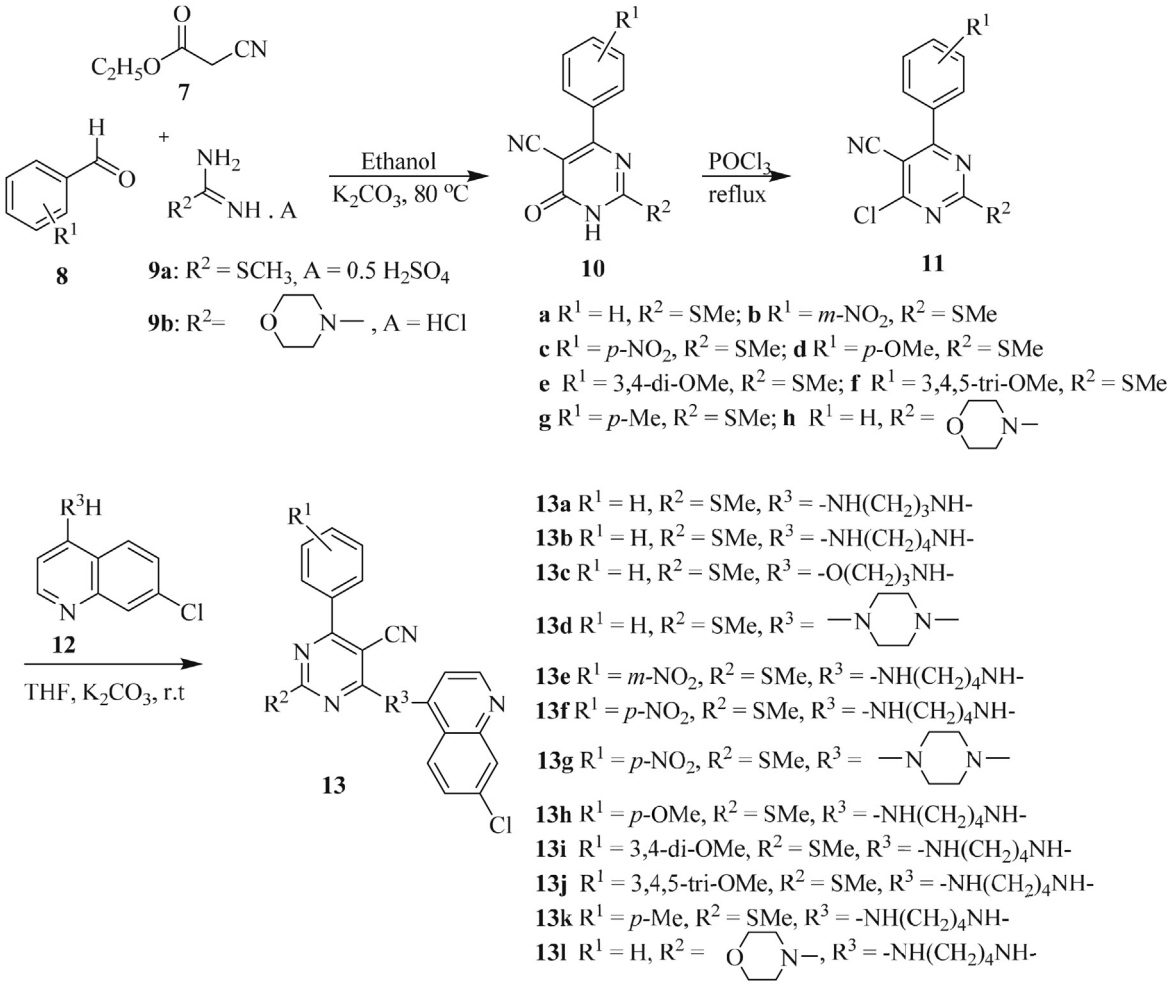

Scheme 1. Synthesis of pyrimidine-5-carbonitrile-quinoline hybrids.

unit, which are known to inhibit cysteine proteases [13–15] and show antiplasmodial effects.

Comparison of the antiplasmodial activity of the hybrids **13b**, **13e**, **13f**, **13h** and **13k** suggested that **13e** [IC_{50} = 68.5 nM (NF54, CQ^S); 55.8 nM (Dd2, CQ^R)] bearing a *m*-nitro substituent at the C-4 phenyl ring showed highest activity against both the *P. falciparum* strains. Moreover, position of the nitro substituent on the aromatic ring also significantly modulated (Table 1) the antiplasmodial activity. Thus, the *m*-NO_2 substituted analog [**13e**: IC_{50} = 68.5 nM (NF54); 55.8 nM (Dd2)] showed superior activity against CQ^R strain, while, a *p*-NO_2 [**13f**: IC_{50} = 43.8 nM (NF54); 531.6 nM (Dd2)] substituted derivate was more active against CQ^S strain. In the case of methoxy substituted hybrids (**13h–j**), all the hybrids depicted good antiplasmodial activity against the CQ^S strain and mild activity against CQ^R strain, except the 3,4,5-trimethoxyphenyl substituted hybrid **13j** [IC_{50} = 90.9 nM (NF54); 89.9 nM (Dd2)], which exhibited 3-fold greater antiplasmodial activity than CQ [IC_{50} = 257.6 nM (Dd2)] against CQ^R strain and is the second most potent [IC_{50} = 90.9 nM (NF54); 89.9 nM (Dd2)] hybrid of the current series of compounds. Furthermore, replacement of the C-2 S-methyl group of the pyrimidine unit in **13b** [IC_{50} = 197.9 nM (NF54); 385.8 nM (Dd2)] by morpholine ring to yield hybrid **13l** [IC_{50} = 108.6 nM (NF54); 295.2 nM (Dd2)] led to a deterioration of antiplasmodial activity against both CQ^S as well as CQ^R strains. The molecular weight of these hybrids is close to 500 and CLog*P* values are in the range 5–7.51 (Table 1). While the selectivity indices (SI) of these hybrids are low, the most active hybrids **13e** (RI = 0.81) and **13j** (RI = 0.98) depicted good resistance index, which is better than the standard antiplasmodial drugs (CQ & ASN, Table 1).

This brief SAR study on the new pyrimidine-quinoline hybrids clearly demonstrated that the antiplasmodial activity of these hybrids was significantly influenced by the cyano group at C-5 position, type and length of the methylene spacer linking pyrimidine and quinoline units as well as the substitution pattern (C-2 as well as C-4 positions) of the pyrimidine unit.

3.2. Cytotoxicity

Cytotoxicity of **13a–l** and reference CQ was evaluated using murine leukemia cells (L1210), human T-lymphocyte cells (CEM) and human cervix carcinoma cells (HeLa). The cytotoxicity data revealed that most of these hybrids except **13d** and **13g** were more cytotoxic than CQ against all the three tested mammalian tumor cell lines (Table 2). Moreover, the SI of all the hybrids [1.9–103.7 (CQ^S); 1.1–44.0(CQ^R)] is lower than CQ [SI = 972.9 (CQ^S); 69.8 (CQ^R)]. However, the SI of the most active hybrids **13e** and **13j**, against CQ^R strain was higher (Table 2) and approached that of CQ. Thus, these hybrids display cytotoxicity (Table 2) only at concentrations that are significantly higher than concentrations at which hybrids displayed antiplasmodial activity.

3.3. Antiviral activity

Antiplasmodial drugs such as CQ, artemisinin, and quinine

Table 1
In vitro antiplasmodial activity of **13a–l** against *P. falciparum* (CQ^S) NF54 strain and (CQ^R) Dd2 strain for n = 3 (n = number of replicates).

Hybrid	Structure	Yield (%)[a]	NF54 IC_{50} (nM)[b,c]	Dd2 IC_{50} (nM)[c,d]	Clog*P*[e]	RI[f]
13a	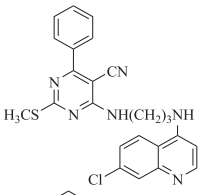	87	133.7 ± 15.7	319.4 ± 101.4	6.90	2.38
13b	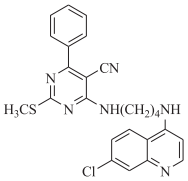	82	108.6 ± 2.2	295.2 ± 19.1	7.02	2.71
13c	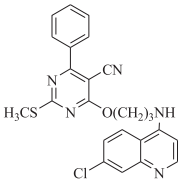	89	88.8 ± 3.4	208.1 ± 83.5	6.89	2.34
13d	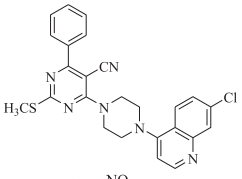	85	131923.2 ± 4.689.5	211819.5 ± 0	5.95	1.60
13e	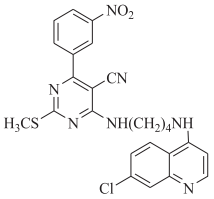	84	68.5 ± 6.0	55.8 ± 4.4	6.77	0.81
13f	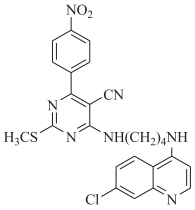	88	43.8 ± 1.2	531.6 ± 29.2	6.77	12.13
13g	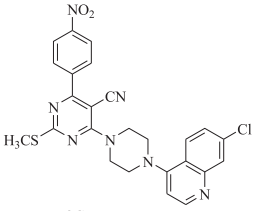	91	12250 ± 445.4	9862.6 ± 2063.4	5.70	0.80
13h	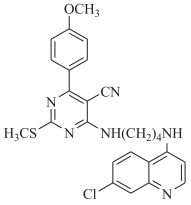	80	109.9 ± 22.4	1529.7 ± 189.6	7.06	13.92
13i		85	192.8 ± 26.1	1283.3 ± 770.3[g]	6.77	6.65

(*continued on next page*)

Table 1 (*continued*)

Hybrid	Structure	Yield (%)[a]	NF54 IC_{50} (nM)[b,c]	Dd2 IC_{50} (nM)[c,d]	ClogP[e]	RI[f]
13j	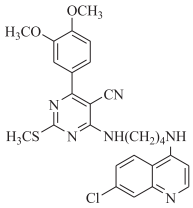	83	90.9 ± 3.3	89.5 ± 9.9	6.47	0.98
13k	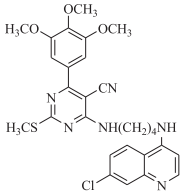	84	119.3 ± 5.3	542.8 ± 22.5	7.51	4.54
13l	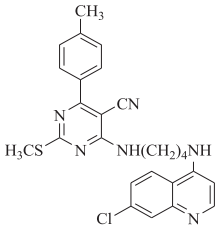	92	197.9 ± 78.3	385.8 ± 99.7	6.35	1.95
CQ			18.5 ± 0.8	257.6 ± 82.8	5.1	13.92
ASN			12.6 ± 2.9	17.4 ± 5.4	1.06	1.38

[a] Yields based on isolated purified products.
[b] CQ sensitive strain.
[c] Data represents the mean of three independent experiment.
[d] CQ resistant strain.
[e] Calculated from ChemDraw Ultra 11.0.
[f] Resistance Index (RI) = IC_{50} (Dd2)/IC_{50}(NF54).
[g] Variability in data is probably due to poor solubility.

inhibit several RNA and DNA viruses [20]. CQ being a weak lysosomotropic base exerts antiviral activity by inhibiting replication of some viruses either through reducing the efficiency of endosome-mediated virus entry or through inhibiting the low pH- dependent proteases in trans-Golgi vesicles [21,22]. Taking into consideration the antiviral activity of CQ, we evaluated antiviral activity of hybrids **13a**–**l** against several viruses such as (i) herpes simplex virus-1 (KOS), herpes simplex virus-2 (G), vaccinia virus, vesicular stomatitis virus, herpes simplex virus-1 (TK^{-}KOS ACV^{r}) and adenovirus using HEL cell cultures (ii) vesicular stomatitis virus, coxsackie virus B4, respiratory syncytial virus in HeLa cell cultures, (iii) parainfluenza-3 virus, reovirus-1, Sindbis virus, Coxsackie virus B4,

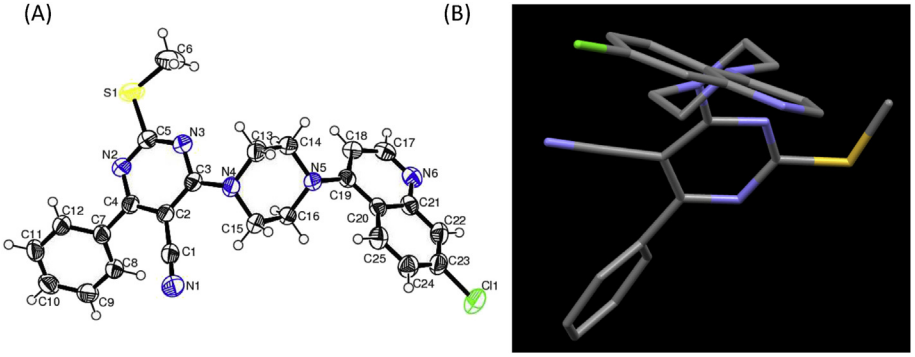

Fig. 2. (A) Ortep diagram of **13d** showing stereo view of the molecule and the numbering scheme used in the structure analysis (CCDC number: 1019022). (B) View showing orientation of piperazinyl ring w.r.t quinoline ring.

Table 2
In vitro cellular toxicity of **13a**–**l** and CQ against murine leukemia cells (L1210), human T-lymphocyte cells (CEM) and human cervix carcinoma cells (HeLa).

Compound	IC_{50} (μM)[a]			SI[b]	SI[c]
	L1210 (μM)	CEM	HeLa		
13a	4.7 ± 0.7	4.7 ± 0.5	11 ± 2	82.3	34.4
13b	4.4 ± 0.4	5.2 ± 1.2	8.5 ± 0.2	78.3	28.7
13c	3.9 ± 0.7	3.3 ± 0.2	3.4 ± 0.1	38.3	16.3
13d	>250	>250	>250	>1.9	>1.1
13e	2.1 ± 1.6	2.1 ± 0.7	1.1 ± 0.1	16.0	19.7
13f	0.96 ± 0.05	0.76 ± 0.06	0.89 ± 0.37	20.3	1.6
13g	206 ± 62	156 ± 21	228 ± 22	18.6	23.1
13h	3.2 ± 0.6	2.7 ± 0.1	3.4 ± 0.1	30.9	2.2
13i	18 ± 3	16 ± 2	20 ± 0	103.7	15.5
13j	3.8 ± 0.8	3.6 ± 0.2	3.4 ± 1.2	37.4	37.9
13k	4.3 ± 0.5	4.9 ± 0.2	5.0 ± 1.4	41.9	9.2
13l	4.2 ± 0.8	4.6 ± 0.3	17 ± 0	86.3	44.0
CQ	15 ± 2	23 ± 4	18 ± 4	972.9	69.8

[a] 50% inhibitory concentration.
[b] Calculated as IC_{50} (HeLa)/IC_{50} (NF54 strain) ratio.
[c] Calculated as IC_{50} (HeLa)/IC_{50} (Dd2 strain) ratio.

Punta Toro virus in Vero cell cultures, (iv) cytomegalovirus using AD-169 and Davis strain in HEL cell cultures, (v) varicella-zoster virus (VZV) in HEL cell cultures (Table S2–S3) and (vi) influenza A virus (H1N1 and H3N2) and influenza B virus in MDCK cell cultures, (Table S2–S3). The data showed that none of the hybrids display any antiviral activity at subtoxic concentrations (Table S2–S3).

3.4. Possible mode of antiplasmodial effects

Malarial parasite invades the host red blood cells and feed on the hemoglobin. The released heme byproduct Fe(III)-protoporphyrin IX, is toxic to the parasite, and is sequestered into physiologically insoluble hemozoin crystals (heme detoxification) [6]. Quinoline drugs form π-π complex with heme ferriprotoporphyrin IX (FPPIX) in FV, and inhibit the formation of hemozoin crystals [6,7]. This inhibition of heme crystallization leads to the accumulation of heme in FV thereby causing parasite death. Thus, quinoline drugs exert antimalarial effect by inhibiting the heme detoxification process. In order to get an insight into the possible mode of action of these hybrids we decided to evaluate the binding of the most potent hybrid **13e** (Table 1) of the current series with monomeric as well as dimeric heme using UV–visible absorption spectrophotometery [16].

The titrations were performed at pH 7.4 as well as 5.6 representing the acidic pH of the food vacuole. The sequential addition of **13e** [pH 7.4: 0–18.3 μM; pH 5.6: 0–52.5 μM (DMSO)] to a solution of monomeric heme in 0.02 M HEPES buffer in aqueous DMSO representing a constant concentration (2.4 μM) showed a substantial decrease in the absorption intensity of the Soret band of Fe(III)PPIX at 402 nm without significant shift in the position of the absorption band (Figs. 3A–4A). This significant hypochromism indicated complexation between Fe(III)PPIX and quinolone unit of **13e**. Further, the Job's plot revealed 1:1 stoichiometry of the most stable complex of **13e** with monomeric heme at pH 7.5 and 5.6 (Figs. 3B–4B).

To ascertain the formation of the proposed complex, mass spectrum of the complex obtained by mixing equimolar solutions of hemin chloride (0.24 mM) and **13e** (0.24 mM) was recorded. The spectrum depicted an intense molecular ion peak at *m/z* 1135.4094 (Fig. 5), corresponding to the molecular formula $C_{59}H_{54}ClFeN_{11}O_6S$ of the 1:1 complex.

Further, it is known that CQ binds to heme dimer (μ-oxo heme) [23] and thus the binding assay was extended to μ-oxo heme also. Titration of μ-oxo heme (10 μM, 0.02 M phosphate buffer) with sequential addition of **13e** (0–13.7 μM) at pH 5.8 showed a decrease in the intensity of the broad peak at 364 nm (Fig. 6A). Further, the Job's plot calculations indicated a 1:1 stoichiometry for the most stable complex of μ-oxo heme and **13e** (Fig. 6B). A similar titration of CQ with heme was also performed under identical conditions, and the association constants were compared (Table 3).

The association constants (Table 3) were calculated from the titration data obtained for monomeric heme (at pH 7.4 and 5.6) and μ-oxo heme using HypSpec, a nonlinear least-squares fitting program [24]. The greater association constants of **13e** with both monomeric (pH 7.4 and pH 5.6) as well as μ-oxo heme compared to CQ (Table 3) suggested stronger complexation of **13e** with heme. Furthermore, the observed trend of the binding of the hybrid with heme (Table 3) suggested stronger binding at the lower pH. The comparison of association constants of **13e** for monomeric and μ-oxo heme revealed that the hybrid has greater affinity for the μ-oxo heme and thus, possibly inhibits hemozoin formation by blocking the growing face of heme leading to the observed antiplasmodial activity. The calculated association constants of **13e** are quite comparable with the hybrids [16] lacking a C-5 carbonitrile, this suggested that the primary mechanism of action of these hybrids is through inhibition of heme polymerization, although the cysteine protease inhibition might be playing a supportive role.

4. Conclusions

Covalently linked hybrids of pyrimidine-5-carbonitrile and 4-aminoquinoline display structure-dependent antiplasmodial

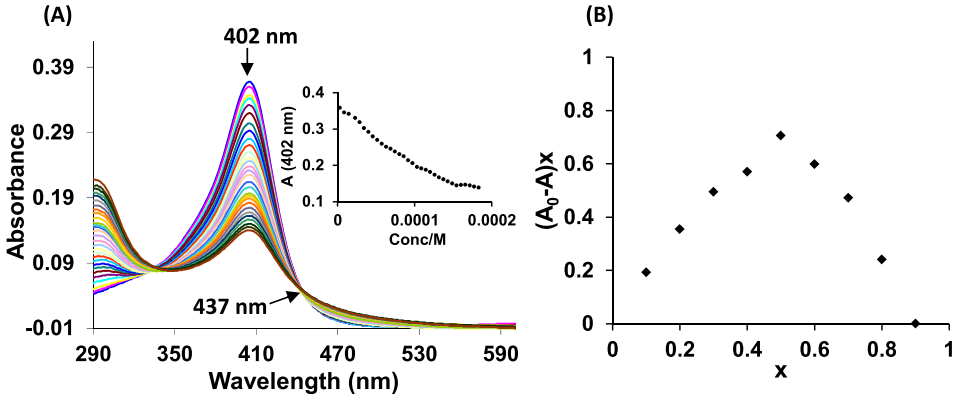

Fig. 3. (A) UV–visible absorption changes in the titration of **13e** with monomeric heme at pH 7.4; (B) Job plot of monomeric heme complex formation at pH 7.4. x = [**13e**]/[**13e**]+[heme] is the mole fraction of the **13e**, A_0 is the absorbance, when x = 1 and A is the absorbance at respective values of x.

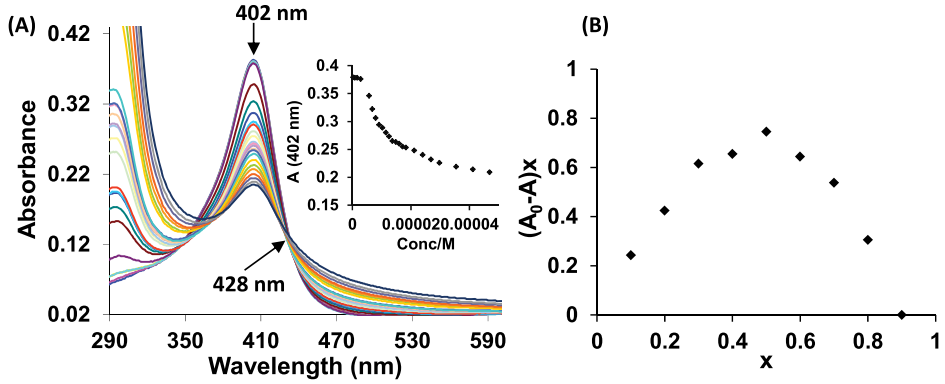

Fig. 4. (A) UV–visible absorption changes in the titration of **13e** with monomeric heme at pH 5.6; (B) Job plot of monomeric heme complex formation at pH 5.6. x = [**13e**]/[**13e**]+[heme] is the mole fraction of the **13e**, A_0 is the absorbance, when x = 1 and A is the absorbance at respective values of x.

activity in nM range, which is superior to the corresponding hybrids lacking the 5-cyano group on the pyrimidine unit. The hybrids possessing a nitrophenyl group at the C-4 position and a SMe group at the C-2 position of the pyrimidine unit are more effective against both CQ-sensitive and CQ-resistant strains. The hybrids **13e** and **13j** showed the highest antiplasmodial activity against the Dd2 (CQ^R) strain. However, the current design of hybrids gave a lower selectivity index compared to CQ. From the heme binding studies, it is concluded that inhibition of hemozoin formation is the primary mechanism of antiplasmodial activity of this class of hybrids, while the cyano substitution seems to play a positive but a supportive role.

5. Experimental

5.1. General information

All liquid reagents were dried/purified following recommended drying agents and/or distilled over 4 Å molecular sieves. THF was dried (Na-benzophenone ketyl) under nitrogen. ^{1}H NMR (300 MHz, 400 MHz and 500 MHz), ^{13}C (75 MHz, 100 MHz and 125 MHz), were recorded in $CDCl_3$ and DMSO-d_6 on a multinuclear Jeol FT-AL-300 spectrometer and BrukerAvance II 400 & III 500 spectrometer with chemical shifts being reported in parts per million (δ) relative to internal tetramethylsilane (TMS, δ 0.0, ^{1}H NMR) or chloroform ($CDCl_3$, δ 77.0, ^{13}C NMR). Mass spectra were recorded on a Bruker LC-MS MICROTOF II spectrometer. Elemental analysis was performed on FLASH EA 112 (Thermo electron Corporation) analyzer and the results are quoted in %. IR spectra were recorded on Perkin Elmer FTIR-C92035 Fourier transform spectrometer in the range 400–4000 cm^{-1} using KBr pellets. For monitoring the progress of a reaction and for comparison purpose, thin layer chromatography (TLC) was performed on pre-coated aluminum sheets of Merck ($60F_{254}$, 0.2 mm) using an appropriate solvent system. The chromatograms were visualized under UV light. For column chromatography silica gel (60–120 mesh) was employed and eluents were ethyl acetate/hexane or ethyl acetate/methanol mixtures. The pH measurements were performed with the Equip-Tronics Digital pH meter model-EQ 610. The purities of all the final compounds were confirmed to be ≥ 95% by combustion methods. UV–visible spectral studies were conducted on Shimadzu 1601 PC spectrophotometer with a quartz cuvette (path length, 1 cm). The absorption spectra have been recorded between 1100 and 200 nm. The cell holder of the spectrophotometer was thermostatted at 25 °C for consistency in the recordings.

5.2. Synthesis of pyrimidin-6(1H)-ones (***10a–h***)

5.2.1. Synthesis of 5-cyano-2-methylthio-4-phenylpyrimidin-6(1H)-one (***10a***)

In a typical procedure, to a solution of *S*-methylisothiourea (1 g, 11.10 mmol), benzaldehyde (2.23 ml, 22.10 mmol), and ethyl cyanoacetate (2.37 ml, 22.10 mmol) in ethanol (40 ml), K_2CO_3 (3.06 g, 22.10 mmol) was added. The reaction mixture was heated to 80 °C for 5 h and filtered after cooling to isolate the corresponding product. Recrystallization from methanol provided **10a** as yellow crystalline solids in 84% yield. Rf: 0.75 (ethyl acetate). m.p. > 250 °C (methanol). IR (KBr): ν_{max} 1469, 1563, 1656, 2195, 3061, 3234 cm^{-1}. ^{1}H NMR (500 MHz, DMSO-d_6, 25 °C): δ 2.35 (s, 3H, SCH_3), 7.45–7.47 (m, 3H, ArH), 7.75 (t, 2H, *J* 5.8 Hz, ArH). ^{13}C NMR (125 MHz, DMSO-

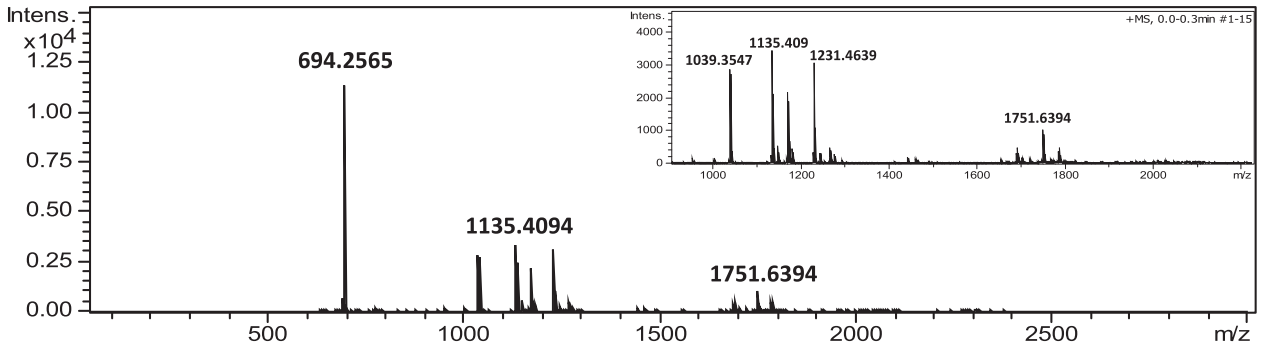

Fig. 5. (A) The solution phase mass spectrum of **13e** (0.24 mmol) upon addition of monomeric heme (0.24 mmol) in 40% aqueous DMSO solution (inset shows zoom between *m/z* 1000 and 2500).

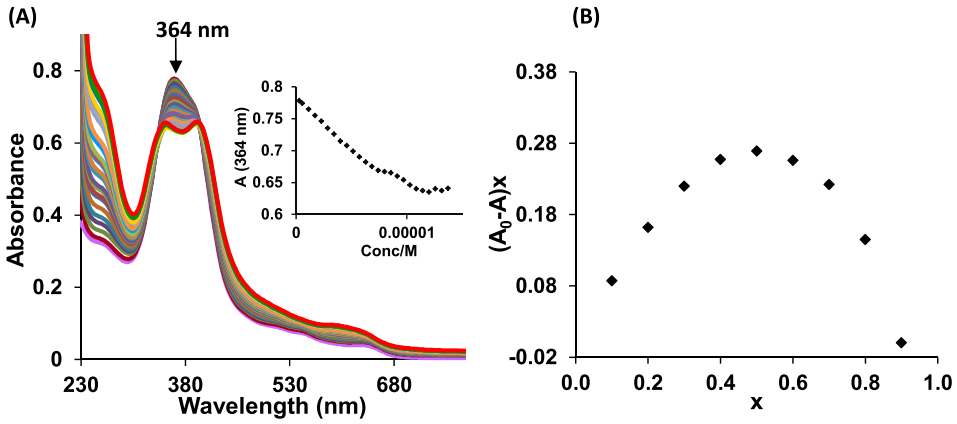

Fig. 6. (A) UV–visible absorption changes in the titration of **13e** with μ-oxo heme at pH 5.8; (B) Job plot of μ-oxo heme complex formation at pH 5.8 x = [**13e**]/[**13e**]+[heme] is the mole fraction of the **13e**, A_0 is the absorbance, when x = 1 and A is the absorbance at respective values of x.

d_6, 25 °C): δ 13.7, 89.0, 120.7, 126.6, 127.4, 128.5, 129.2, 130.0, 138.1, 167.3, 170.9 and 172.9. Anal. Calcd. for $C_{12}H_9N_3OS$: C, 59.26; H, 3.70; N, 17.28, S, 13.18. Found: C, 59.31; H, 3.80; N, 17.19, S, 13.30. EIMS: *m/z* 244 $(M + H)^+$. UV/vis (DMSO): λ_{max} (ε/L mol^{-1} cm^{-1}) 328 nm (57900).

Following the above procedure and using appropriate aldehyde, **10b–g** were analogously prepared. For the preparation of **10h**, condensation of benzaldehyde, ethyl cyanoacetate and N-morpholinyl guanidine hydrochloride was performed. The experimental details as well as characteristic data of **10b–h** are presented in the Supplementary Data.

5.3. Synthesis of 4-aryl-5-cyano-6-chloro-2-methylthiopyrimidines (*11a–h*)

5.3.1. Synthesis of 5-cyano-6-chloro-2-(methylthio)-4-phenylpyrimidine (*11a*)

A suspension of **10a** (0.50 g, 2.05 mmol) in distilled $POCl_3$ (5 ml, 53.80 mmol) was heated at 105 °C for 3 h and the excess $POCl_3$ was removed under reduced pressure. The residue was purified by column chromatography (60–120 mesh silica) using ethyl acetate/hexane as chromatograpic eluent (1:9 *v/v*) to obtain the product as white solid in 97% yield. Rf: 0.74 [ethyl acetate:hexane/1:4 (*v/v*)]. m.p. 110 °C (dichloromethane/hexane). IR (KBr): ν_{max} 1474, 1537, 2228, 3066 cm^{-1}. ^{1}H NMR (500 MHz, $CDCl_3$, 25 °C): δ 2.66 (s, 3H, SCH_3), 7.52–7.54 (m, 3H, ArH), 8.03 (d, 2H, *J* 10.0 Hz, ArH). ^{13}C NMR (125 MHz, $CDCl_3$, 25 °C): δ 14.7, 100.7, 114.6, 128.5, 128.9, 129.2, 130.1, 132.5, 134.3, 163.5, 168.5, and 176.4. Anal. Calcd. for $C_{12}H_8ClN_3S$: C, 55.17; H, 3.06; N, 16.09, S, 12.25. Found: C, 55.22; H, 3.11; N, 16.17; S, 12.34. EIMS: *m/z* 261 (M^+). UV/vis (CH_2Cl_2): λ_{max} (ε/L mol^{-1} cm^{-1}) 286 nm (9160).

Following the similar procedures and using appropriate **10b–h**, **11b–h** were analogously prepared. The experimental details as well as characteristic data of **10b–h** are presented in the Supplementary Data.

5.4. General procedure for the synthesis of pyrimidine-5-carbonitrile-quinoline hybrids

The solution of appropriate 4-aminoquinoline **12** (3.38 mmol) in dry THF (10 ml) was added to the stirred solution of **11** (1.69 mmol) and potassium carbonate (8.45 mmol) in dry THF (20 ml). The reaction mixture was stirred at room temperature for 48 h and upon completion (TLC), the reaction mixture was filtered and the filtrate was concentrated under vacuum. The residue was purified by column chromatography over 60–120 mesh silica using hexane/ethyl acetate or ethyl acetate/methanol (**13a–l**) as eluent. Using this procedure, the following compounds were isolated.

5.4.1. 2-Methylthio-4-phenyl-6-[(7-chloroquinolin-4-yl) aminopropyl]aminopyrimidine-5-carbonitrile (*13a*)

Chromatograpic eluent: ethyl acetate/methanol (99:1 *v/v*). White solid. Rf: 0.40 (ethyl acetate). Yield: 87%. m.p. 205–207 °C (dichloromethane/hexane). IR (KBr): ν_{max} 1583, 2209, 2935, 3343 cm^{-1}. ^{1}H NMR (300 MHz, $CDCl_3$, 25 °C): δ 2.06 (t, 2H, *J* 6.0 Hz, CH_2), 2.58 (s, 3H, SCH_3), 3.46 (t, 2H, *J* 6.0 Hz, CH_2), 3.74–3.81 (m, 2H, CH_2), 5.55 (br, 1H, D_2O exchangeable, NH), 5.87 (br, 1H, D_2O exchangeable, NH), 6.44 (d, 1H, *J* 5.4 Hz, ArH), 7.38 (dd, 1H, *J* 2.4 Hz, 6.6 Hz, ArH), 7.48–7.52 (m, 3H, ArH), 7.87 (d, 1H, *J* 9.0 Hz, ArH), 7.95–7.98 (m, 3H, ArH), 8.53 (d, 1H, *J* 5.1 Hz, ArH). ^{13}C NMR (75 MHz, $CDCl_3$, 25 °C): δ 14.0, 27.5, 42.0, 42.2, 83.5, 99.1, 116.8, 117.9, 124.4, 127.8, 128.9, 131.4, 133.8, 136.4, 149.4, 150.4, 152.2, 161.6, 167.3 and 174.4. Anal. Calcd. for $C_{24}H_{21}ClN_6S$: C, 62.60; H, 4.56; N, 18.26, S, 6.95. Found: C, 62.41; H, 4.64; N, 18.13; S, 6.88. EIMS: *m/z* 461 $(M + H)^+$. UV/vis (CH_2Cl_2): λ_{max} (ε/L mol^{-1} cm^{-1}) 254 nm (39198), 324 nm (15040).

5.4.2. 2-Methylthio-4-phenyl-6-[(7-chloroquinolin-4-yl) aminobutyl]aminopyrimidine-5-carbonitrile (*13b*)

Chromatograpic eluent: ethyl acetate/methanol (99:1 *v/v*). White solid. Rf: 0.50 (ethyl acetate). Yield: 82%. m.p. 160–162 °C

Table 3
Binding constants (log *K*) of **13e** and CQ with heme and μ-oxoheme.

Compound	Monomeric heme log $K \pm \sigma$		μ-oxo heme log $K \pm \sigma$
	pH 5.6	pH 7.5	pH 5.8
13e	5.54 ± 0.03	5.08 ± 0.01	5.86 ± 0.07
CQ	4.65 ± 0.02	5.15 ± 0.10	5.58 ± 0.08
Stoichiometry	1:1	1:1	1:1

(dichloromethane/hexane). IR (KBr): ν_{max} 1578, 2213, 2927, 3060, 3282 cm^{-1}. ^1H NMR (300 MHz, $CDCl_3$, 25 °C): δ 1.87–1.92 (m, 4H, 2 × CH_2), 2.56 (s, 3H, SCH_3), 3.42–3.45 (m, 2H, CH_2), 3.60–3.69 (m, 2H, CH_2), 5.03 (br, 1H, D_2O exchangeable, NH), 5.74 (br, 1H, D_2O exchangeable, NH), 6.44 (d, 1H, *J* 5.1 Hz, ArH), 7.36 (d, 1H, *J* 2.1 Hz, ArH), 7.39–7.53 (m, 3H, ArH), 7.68 (d, 1H, *J* 9.0 Hz, ArH), 7.95–7.97 (m, 3H, ArH), 8.55 (d, 1H, *J* 5.4 Hz, ArH). ^{13}C NMR (75 MHz, $CDCl_3$, 25 °C): δ 14.0, 25.5, 26.5, 41.0, 42.5, 79.6, 83.3, 99.1, 116.7, 117.9, 124.4, 124.5, 127.9, 128.9, 131.4, 133.8, 136.4, 149.5, 150.5, 152.3, 161.5, 167.3 and 174.4. Anal. Calcd. for $C_{25}H_{23}ClN_6S$: C, 63.29; H, 4.85; N, 17.72; S, 6.75. Found: C, 63.14; H, 4.72; N, 17.64; S, 6.67. EIMS: *m/z* 475 $(M + H)^+$. UV/vis (CH_2Cl_2): λ_{max} (ε/L mol^{-1} cm^{-1}) 252 nm (23710), 324 nm (7210).

5.4.3. 2-Methylthio-4-phenyl-6-[(7-chloroquinolin-4-yl) aminopropoxy]pyrimidine-5-carbonitrile **(13c)**

Chromatograpic eluent: ethyl acetate/methanol (99:1 *v/v*). White solid. Rf: 0.50 (ethyl acetate). Yield: 89%. m.p. 138–140 °C (dichloromethane/hexane). IR (KBr): ν_{max} 1332, 1580, 2220, 3061, 3212 cm^{-1}.^1H NMR (300 MHz, $CDCl_3$, 25 °C): δ 2.29–2.33 (m, 2H, CH_2), 2.62 (s, 3H, SCH_3), 3.59–3.62 (m, 2H, CH_2), 4.72 (t, 2H, *J* 5.4 Hz, CH_2), 5.40 (br, 1H, D_2O exchangeable, NH), 6.49 (d, 1H, *J* 5.1 Hz, ArH), 7.39 (dd, 1H, *J* 2.1 Hz, 9.0 Hz, ArH), 7.42–7.56 (m, 3H, ArH), 7.82 (d, 1H, *J* 9.0 Hz, ArH), 7.95 (d, 1H, *J* 1.8 Hz, ArH), 8.06–8.03 (m, 2H, ArH), 8.55 (d, 1H, *J* 5.7 Hz, ArH). ^{13}C NMR (75 MHz, $CDCl_3$, 25 °C): δ 14.4, 27.7, 40.2, 66.5, 100.1, 115.4, 116.3, 121.3, 125.6, 128.8, 128.9, 131.9, 135.2, 148.4, 150.3, 152.6, 165.3, 168.5 and 173.2. Anal. Calcd. for $C_{24}H_{20}ClN_5OS$: C, 62.47; H, 4.33; N, 15.18; S, 6.94. Found: C, 62.54; H, 4.31; N, 15.11; S, 6.90. EIMS: *m/z* 462 $(M + H)^+$. UV/vis (CH_2Cl_2): λ_{max} (ε/L mol^{-1} cm^{-1}) 252 nm (10780), 312 nm (3280).

5.4.4. 2-Methylthio-4-phenyl-6-[1-(7-chloroquinolin-4-yl] piperazin-4-yl]pyrimidine-5-carbonitrile **(13d)**

Chromatograpic eluent: ethyl acetate/hexane (80:20 *v/v*).White solid. Rf: 0.87 (ethyl acetate). Yield: 85%. m.p. 188–190 °C (dichloromethane/hexane). IR (KBr): ν_{max} 1578, 2206, 2822, 2924, 3035 cm^{-1}. ^1H NMR (300 MHz, $CDCl_3$, 25 °C): δ 2.59 (s, 3H, SCH_3), 3.38 (t, 4H, *J* 4.8 Hz, 2 × CH_2), 4.27 (t, 4H, *J* 4.8 Hz, 2 × CH_2), 6.88 (d, 1H, *J* 4.8 Hz, ArH), 7.46–7.57 (m, 4H, ArH), 7.89 (dd, 2H, *J* 1.5 Hz, 6.3 Hz, ArH), 7.98 (d, 1H, *J* 9.0 Hz, ArH), 8.08 (d, 1H, *J* 2.1 Hz, ArH), 8.76 (d, 1H, *J* 4.8 Hz, ArH). ^{13}C NMR (75 MHz, $CDCl_3$, 25 °C): δ 14.4, 47.2, 51.9, 84.1, 109.3, 118.3, 124.7, 126.6, 128.5, 129.0, 129.3, 131.4, 135.2, 136.1, 150.1, 151.9, 156.1, 162.9, 170.8 and 174.5. Anal. Calcd. for $C_{25}H_{21}ClN_6S$: C, 63.55; H, 4.44; N, 17.79; S, 6.77. Found: C, 63.61; H, 4.34; N, 17.71; S, 6.70. EIMS: *m/z* 473 $(M + H)^+$. UV/vis (CH_2Cl_2): λ_{max} (ε/L mol^{-1} cm^{-1}) 252 nm (14890), 329 nm sh (2330).

5.4.5. 2-Methylthio-4-(m-nitrophenyl)-6-[(7-chloroquinolin-4-yl) aminobutyl]aminopyrimidine-5-carbonitrile **(13e)**

Chromatograpic eluent: ethyl acetate/hexane (90:10 *v/v*).Yellow solid. Rf: 0. 34 (ethyl acetate). Yield: 84%. m.p. 155–157 °C (dichloromethane/hexane). IR (KBr): ν_{max} 1347, 1583, 1725, 2202, 3056, 3360 cm^{-1}. ^1H NMR (300 MHz, $CDCl_3$, 25 °C): δ 1.86–1.88 (m, 4H, 2 × CH_2), 2.69 (s, 3H, SCH_3), 3.40–3.43 (m, 2H, CH_2), 3.70–3.72 (m, 2H, CH_2), 5.01 (br, 1H, D_2O exchangeable, NH), 5.82 (br, 1H, D_2O exchangeable, NH), 6.44 (d, 1H, *J* 5.7 Hz, ArH), 7.38 (dd, 1H, *J* 2.1 Hz, 4.5 Hz, ArH), 7.69 (dd, 1H, *J* 7.1 Hz, 13.8 Hz, ArH), 7.96 (d, 1H, *J* 2.1 Hz, ArH), 8.29 (d, 1H, *J* 7.1 Hz, ArH), 8.38 (d, 2H, *J* 7.2 Hz, ArH), 8.55 (d, 1H, *J* 5.4 Hz, ArH), 8.82 (s, 1H, ArH). ^{13}C NMR (75 MHz, $CDCl_3$, 25 °C): δ 13.6, 24.9, 25.9, 40.5, 42.1, 83.0, 96.9, 98.5, 115.6, 117.3, 123.1, 123.7, 123.8, 125.1, 127.1, 129.8, 133.6, 134.4, 137.4, 147.6, 150.2, 151.3, 160.8, 164.2 and 174.3. Anal. Calcd. for $C_{25}H_{22}ClN_7O_2S$: C, 57.80; H, 4.23; N, 18.88, S, 6.16; Found: C, 57.68; H, 4.23; N, 18.89; S, 6.27 . EIMS: *m/z* 520 $(M + H)^+$. UV/vis (CH_2Cl_2): λ_{max} (ε/L mol^{-1} cm^{-1}) 252 nm (15770), 326 nm (3350).

5.4.6. 2-Methylthio-4-(p-nitrophenyl)-6-[(7-chloroquinolin-4-yl) aminobutyl]aminopyrimidine-5-carbonitrile **(13f)**

Chromatograpic eluent: ethyl acetate/hexane (90:10 *v/v*). Yellow solid. Rf: 0.45 (ethyl acetate). Yield: 88%. m.p. 150–152 °C (dichloromethane/hexane). IR (KBr): ν_{max} 1351, 1547, 1580, 2208, 2927, 3065, 3335 cm^{-1}. ^1H NMR (300 MHz, $CDCl_3$, 25 °C): δ 1.86–1.91 (m, 4H, 2 × CH_2), 2.57 (s, 3H, SCH_3), 3.42–3.44 (m, 2H, CH_2), 3.71–3.73 (m, 2H, CH_2), 6.43 (d, 1H, *J* 5.4 Hz, ArH), 7.37 (dd, 1H, *J* 2.4 Hz, 9.0 Hz, ArH), 7.68 (d, 1H, *J* 2.4 Hz, ArH), 7.96 (d, 1H, *J* 2.1 Hz, ArH), 8.10 (dd, 2H, *J* 1.8 Hz, 9.0 Hz, ArH), 8.35 (dd, 2H, *J* 1.8 Hz, 6.0 Hz, ArH), 8.53 (d, 1H, *J* 5.4 Hz, ArH). ^{13}C NMR (75 MHz, $CDCl_3$, 25 °C): δ 13.6, 24.9, 25.9, 40.5, 42.0, 98.3, 101.5, 117.4, 123.3, 123.8, 127.1, 129.8, 133.5, 141.8, 148.5, 150.2, 151.3, 160.8 and 174.3. Anal. Calcd. for $C_{25}H_{22}ClN_7O_2S$: C, 57.80; H, 4.23; N, 18.88, S, 6.16; Found: C, 57.68; H, 4.23; N, 18.89; S 6.27. EIMS: *m/z* 520 $(M + H)^+$. UV/vis (CH_2Cl_2): λ_{max} (ε/L mol^{-1} cm^{-1}) 252 nm (19840), 320 nm (4630).

5.4.7. 2-Methylthio-4-(p-nitrophenyl)-6-[1-(7-chloroquinolin-4-yl] piperazin-4-ylpyrimidine-5-carbonitrile **(13g)**

Chromatograpic eluent: ethyl acetate/hexane (80:20 *v/v*). White solid. Rf: 0.54 (ethyl acetate). Yield: 91%. m.p. 190 °C (dichloromethane/hexane). IR (KBr): ν_{max} 1423, 1533, 2210, 2923, 3039 cm^{-1}. ^1H NMR (300 MHz, $CDCl_3$, 25 °C): δ 2.59 (s, 3H, SCH_3), 3.50–3.52 (m, 4H, 2 × CH_2), 4.30–4.33 (m, 4H, 2 × CH_2), 6.92 (d, 1H, *J* 5.4 Hz, ArH), 7.52 (dd, 1H, *J* 2.0 Hz, 9.0 Hz, ArH), 7.98–8.07 (m, 3H, ArH), 8.19 (s, 1H, ArH), 8.35 (d, 2H, *J* 9.0 Hz, ArH), 8.75 (d, 1H, *J* 5.1 Hz, ArH). ^{13}C NMR (75 MHz, $CDCl_3$, 25 °C): δ 13.5, 14.1, 29.5, 29.7, 46.9, 51.6, 123.4, 126.9, 130.3 and 152.2. Anal. Calcd. for $C_{25}H_{20}ClN_7O_2S$: C, 58.02; H, 3.86; N, 18.95; S, 6.19. Found: C, 57.91; H, 4.00; N, 18.90; S, 6.19. EIMS: *m/z* 518 $(M + H)^+$. UV/vis (CH_2Cl_2): λ_{max} (ε/L mol^{-1} cm^{-1}) 252 nm (15690), 323 nm sh (4678).

5.4.8. 2-Methylthio-4-(p-methoxylphenyl)-6-[(7-chloroquinolin-4-yl)aminobutyl]aminopyrimidine-5-carbonitrile **(13h)**

Chromatograpic eluent: ethyl acetate/hexane (80:20 *v/v*). Yellow solid. Rf: 0.46 (ethyl acetate). Yield: 80%. m.p. 145–147 °C (dichloromethane/hexane). IR (KBr): ν_{max} 1050, 1259, 1566, 2210, 2948, 3309 cm^{-1}. ^1H NMR (300 MHz, $CDCl_3$, 25 °C): δ 1.77–1.79 (m, 4H, 2 × CH_2), 2.48 (s, 3H, SCH_3), 3.30–3.33 (m, 2H, CH_2), 3.60–3.62 (m, 2H, CH_2), 3.80 (s, 3H, OCH_3), 5.00 (br, 1H, D_2O exchangeable, NH), 5.70 (br, 1H, D_2O exchangeable, NH), 6.36 (d, 1H, *J* 5.4 Hz, ArH), 6.93 (d, 2H, *J* 9.0 Hz, ArH), 7.30 (d, 1H, *J* 7.2 Hz, ArH), 7.60 (d, 1H, *J* 8.7 Hz, ArH), 7.95–7.89 (m, 3H, ArH), 8.47 (d, 1H, *J* 5.1 Hz, ArH). ^{13}C NMR (75 MHz, $CDCl_3$, 25 °C): δ 16.7, 28.4, 29.4, 32.1, 45.1, 57.9, 101.5, 116.4, 123.3, 127.9, 131.2, 132.9 and 154.4. Anal. Calcd. for $C_{26}H_{25}ClN_6OS$: C, 61.90; H, 4.96; N, 16.66, S, 6.34. Found: C, 61.74; H, 5.03; N, 16.71; S, 6.43. EIMS: *m/z* 505 $(M + H)^+$. UV/vis (CH_2Cl_2): λ_{max} (ε/L mol^{-1} cm^{-1}) 252 nm (13940), 310 nm (7140).

5.4.9. 2-Methylthio-4-(3,4-dimethoxylphenyl)-6-[(7-chloroquinolin-4-yl)aminobutyl] aminopyrimidine-5-carbonitrile **(13i)**

Chromatograpic eluent: ethyl acetate/hexane (85:15 *v/v*). Yellow solid. Rf: 0.39 (ethyl acetate). Yield: 85%. m.p. 108 °C (dichloromethane/hexane). IR (KBr): ν_{max} 1022, 1262, 1489, 1581, 2202, 2963, 3351 cm^{-1}. ^1H NMR (300 MHz, $CDCl_3$, 25 °C): δ 1.72–1.75 (m, 4H, 2 × CH_2), 2.45 (s, 3H, SCH_3), 3.29–3.31 (m, 2H, CH_2), 3.57–3.59 (m, 2H, CH_2), 3.84 (d, 6H, *J* 3.0 Hz, 2 × OCH_3), 5.05 (br, 1H, D_2O exchangeable, NH), 5.70 (br, 1H, D_2O exchangeable, NH), 6.31 (d, 1H, *J* 5.4 Hz, ArH), 6.85 (d, 1H, *J* 8.4 Hz, ArH), 7.26 (t, 1H, *J* 6.9 Hz, ArH), 7.47 (d, 1H, *J* 2.1 Hz, ArH), 7.57–7.60 (m, 2H, ArH), 7.85 (d, 1H, *J* 2.1 Hz, ArH), 8.41 (d, 1H, *J* 5.1 Hz, ArH). ^{13}C NMR (75 MHz, $CDCl_3$, 25 °C): δ 13.1, 24.9, 26.3, 28.6, 40.4, 44.9, 55.0, 98.2, 110.4, 118.1, 121.3, 127.3, 147.1, 151.3, 160.3, 162.3 and 176.1. Anal. Calcd. for $C_{27}H_{27}ClN_6O_2S$: C, 60.67; H, 5.05; N, 15.73, S, 5.99. Found: C, 60.68;

H, 5.04; N, 15.62; S, 5.94. EIMS: *m/z* 535 $(M + H)^+$. UV/vis (CH_2Cl_2): λ_{max} (ε/L mol^{-1} cm^{-1}) 252 nm (18390), 322 nm (13280).

5.4.10. 2-Methylthio-4-(3,4,5-trimethoxylphenyl)-6-[(7-chloroquinolin-4-yl)aminobutyl] aminopyrimidine-5-carbonitrile (13j)

Chromatograpic eluent: ethyl acetate/hexane (90:10 *v/v*). Yellow solid. Rf: 0.37 (ethyl acetate). Yield: 83%. m.p. 100–102 °C (dichloromethane/hexane). IR (KBr): ν_{max} 1220, 1487, 1581, 2204, 2934, 3106, 3341 cm^{-1}. ^1H NMR (300 MHz, $CDCl_3$, 25 °C): δ 1.87–1.90 (m, 4H, 2 × CH_2), 2.50 (s, 3H, SCH_3), 3.40–3.42 (m, 2H, CH_2), 3.69–3.71 (m, 2H, CH_2), 3.91 (s, 9H, 3 × OCH_3), 5.88 (br, 1H, D_2O exchangeable, NH), 6.04 (br, 1H, D_2O exchangeable, NH), 6.34 (d, 1H, *J* 5.7 Hz, ArH), 7.32 (d, 1H, *J* 2.4 Hz, ArH), 7.35 (d, 1H, *J* 2.1 Hz, ArH), 7.80 (d, 2H, ArH), 7.92 (d, 1H, *J* 2.1 Hz, ArH), 8.40 (d, 1H, *J* 5.7 Hz, ArH). ^{13}C NMR (75 MHz, $CDCl_3$, 25 °C): δ 14.3, 25.7, 26.9, 40.9, 42.9, 56.3, 60.9, 82.8, 98.4, 99.9, 106.1, 116.5, 117.1, 122.3, 125.7, 125.9, 130.9, 136.0, 140.8, 148.9, 151.2, 153.1, 161.9, 166.1, 175.1 and 177.1. Anal. Calcd. for $C_{28}H_{29}ClN_6O_3S$: C, 59.57; H, 5.14; N, 14.89, S, 5.67. Found: C, 59.50; H, 5.09; N, 14.80; S, 5.69. EIMS: *m/z* 565 $(M + H)^+$. UV/vis (CH_2Cl_2): λ_{max} (ε/L mol^{-1} cm^{-1}) 252 nm (16970), 320 nm (9340).

5.4.11. 2-Methylthio-4-(p-methylphenyl)-6-[(7-chloroquinolin-4-yl)aminobutyl]aminopyrimidine-5-carbonitrile (13k)

Chromatograpic eluent: ethyl acetate/hexane (90:10 *v/v*). Yellow solid. Rf: 0.42 (ethyl acetate). Yield: 84%. m.p. 153–155 °C (dichloromethane/hexane). IR (KBr): ν_{max} 1577, 2203, 2926, 3244 cm^{-1}. ^1H NMR (300 MHz, $CDCl_3$, 25 °C): δ 1.81–1.86 (m, 4H, 2 × CH_2), 2.43 (d, 3H, *J* 3.6 Hz, CH_3), 2.57 (s, 3H, SCH_3), 3.42–3.44 (m, 2H, CH_2), 3.66–3.70 (m, 2H, CH_2), 5.72 (br, 1H, D_2O exchangeable, NH), 6.43 (d, 1H, *J* 5.4 Hz, ArH), 7.68 (d, 1H, *J* 8.7 Hz, ArH), 7.86–7.89 (m, 5H, ArH), 7.96 (d, 1H, *J* 2.1 Hz, ArH), 8.53 (d, 1H, *J* 5.1 Hz, ArH). ^{13}C NMR (75 MHz, $CDCl_3$, 25 °C): δ 13.6, 21.0, 24.9, 26.1, 40.2, 42.2, 82.4, 98.3, 116.4, 117.4, 123.8, 127.1, 128.3, 128.7, 133.1, 133.5, 140.8, 150.2, 151.3, 161.2 and 173.8. Anal. Calcd. for $C_{26}H_{25}ClN_6S$: C, 63.86; H, 5.15; N, 17.18, S, 6.56; Found: C, 63.79; H, 5.09; N, 17.11; S, 6.49. EIMS: *m/z* 489 $(M + H)^+$. UV/vis (CH_2Cl_2): λ_{max} (ε/L mol^{-1} cm^{-1}) 254 nm (36200), 329 nm (12960).

5.4.12. 2-(Morpholin-4-yl)-4-phenyl-6-[(7-chloroquinolin-4-yl) aminobutyl]aminopyrimidine-5-carbonitrile (13l)

Chromatograpic eluent: ethyl acetate/hexane (90:10 *v/v*). White solid. Rf: 0.40 (ethyl acetate). Yield: 92%. m.p. 178–18 °C (dichloromethane/hexane). IR (KBr): ν_{max} 1443, 2204, 2965, 3340 cm^{-1}. ^1H NMR (500 MHz, $CDCl_3$, 25 °C): δ 1.80–1.86 (m, 4H, 2 × CH_2), 3.40–3.42 (m, 2H, CH_2), 3.63–3.65 (m, 2H, CH_2), 3.74–3.78 (m, 4H, 2 × CH_2), 3.88–3.92 (m, 4H, 2 × CH_2), 5.02 (br, 1H, D_2O exchangeable, NH), 5.55 (br, 1H, D_2O exchangeable, NH), 6.44 (d, 1H, *J* 5.1 Hz, ArH), 7.38 (d, 1H, *J* 7.3 Hz, ArH), 7.49–7.51 (m, 3H, ArH), 7.67 (d, 1H, *J* 8.9 Hz, ArH), 7.93–7.98 (m, 3H, ArH), 8.55 (d, 1H, *J* 5.7 Hz, ArH). ^{13}C NMR (125 MHz, $CDCl_3$, 25 °C): δ 26.2, 27.0, 40.6, 42.9, 44.2, 66.7, 99.0, 116.9, 118.5, 120.7, 125.5, 128.3, 128.4, 128.5, 128.7, 130.8, 135.0, 137.0, 148.7, 148.9, 149.6, 151.8, 160.4, 163.5 and 168.5. Anal. Calcd. for $C_{28}H_{28}ClN_7O$: C, 65.49; H, 5.45; N, 19.10; Found: C, 65.41; H, 5.60; N, 19.01. EIMS: *m/z* 514 $(M + H)^+$. UV/vis (CH_2Cl_2): λ_{max} (ε/L mol^{-1} cm^{-1}) 252 nm (13020), 326 nm (3380).

6. Material and methods for biological activity determination

6.1. In vitro antimalarial activity assay

The test samples were tested in triplicate on one or two separate occasions against chloroquine sensitive (CQ^S) NF54 and chloroquine-resistant (CQ^R) Dd2 strains of *P. falciparum*. Continuous *in vitro* cultures of asexual erythrocyte stages of *P. falciparum* were maintained using a modified method of Trager and Jensen [25]. Quantitative assessment of antiplasmodial activity *in vitro* was determined *via* the parasite lactate dehydrogenase assay using a modified method described by Makler [26].

The test samples were prepared to a 20 mg/ml stock solution in 100% DMSO. Samples were tested as a suspension. Stock solutions were stored at −20 °C. Further dilutions were prepared on the day of the experiment. Chloroquine (CQ) and artesunate were used as the reference drugs in all experiments. A full dose–response was performed for all compounds to determine the concentration inhibiting 50% of parasite growth (IC_{50}–value). Test samples were tested at a starting concentration of 100 μg/ml, which was then serially diluted 2-fold in complete medium to give 10 concentrations; with the lowest concentration being 0.2 μg/ml. The same dilution technique was used for all samples. Reference drugs were tested at a starting concentration of 1000 ng/ml. Active samples were tested at a starting concentration of 1000 ng/ml. The highest concentration of solvent to which the parasites were exposed to had no measurable effect on the parasite viability (data not shown). The IC_{50}-values were obtained using a non-linear dose response curve fitting analysis *via* Graph Pad Prism v.4.0 software.

6.2. Cytotoxicity and antiviral activity assays

Cytotoxicity was determined by exposing different concentrations of the samples to murine leukemia cells (L1210) and human T-lymphocyte cells (CEM) and human cervix carcinoma cells (HeLa) [16]. The cytotoxic activity was determined by measuring the 50% cytotoxic concentration of a compound that inhibited tumor cell proliferation by 50% as measured by a Coulter counter. The antiviral assays were based on inhibition of virus-induced cytopathicity in HEL [herpes simplex virus type 1 (HSV-1), HSV-2 (G), vaccinia virus, adenovirus 3 and vesicular stomatitis virus], Vero (parainfluenza-3, reovirus-1, Coxsackie B4, and Punta Toro virus), HeLa (vesicular stomatitis virus, Coxsackie virus B4, and respiratory syncytial virus) and MDCK (influenza A (H1N1; H3N2) and B virus) cell cultures. Confluent cell cultures in microtiter 96-well plates were inoculated with 100 cell culture inhibitory dose-50 ($CCID_{50}$) of virus (1 $CCID_{50}$ being the virus dose to infect 50% of the cell cultures) in the presence of varying concentrations of the test compounds. Viral cytopathicity was recorded as soon as it reached completion in the control virus-infected cell cultures that were not treated with the test compounds. The cytotoxicity was microscopically determined or examined with the viability staining (MTT) method.

Acknowledgments

We gratefully acknowledge financial assistance from CSIR, New Delhi. H.K. thanks CSIR, New Delhi for senior research fellowship (F. No. 09/254 (0195)/2009-EMR-I). The research of JB was supported by the KU Leuven (GOA 15/19 TBD).

Appendix A. Supplementary data

Supplementary data related to this article can be found at http://dx.doi.org/10.1016/j.ejmech.2015.06.024.

References

[1] WHO, World Malaria Report, 2014. http://www.who.int/malaria/publications/world_malaria_report_2014/en/.
[2] D.A. Fidock, Drug discovery: priming the antimalarial pipeline, Nature 465 (2010) 297–298.
[3] E.H. Ekland, D.A. Fidock, *In vitro* evaluations of antimalarial drugs and their relevance to clinical outcomes, Int. J. Parasitol. 38 (2008) 743–747.

[4] M. Wisniewski, D.J. Zak, Achievements and perspectives of research into development of a vaccine against malaria, Wiad. Parazytol. 56 (2010) 133–140.

[5] A.M. Dondorp, F. Nosten, P. Yi, D. Das, A.P. Phyo, J. Tarning, K.M. Lwin, F. Ariey, W. Hanpithakpong, S.J. Lee, P. Ringwald, K. Silamut, M. Imwong, K. Chotivanich, P. Lim, T. Herdman, S.S. An, S. Yeung, P. Singhasivanon, N.P. Day, N. Lindegardh, D. Socheat, N.J. White, Artemisinin resistance in plasmodium falciparum malaria, N. Engl. J. Med. 361 (2009) 455–467.

[6] M. Foley, L. Tilley, Quinoline antimalarials: mechanisms of action and resistance, Int. J. Parasitol. 27 (1997) 231–240.

[7] L. Tilley, P. Loria, M. Foley, Chloroquine and other quinoline antimalarials, in: P.J. Rosenthal (Ed.), Antimalarial Chemotherapy: Mechanisms of Action, Resistance, and New Directions in Drug Discovery, Humana Press, Totowa, NJ, 2001.

[8] R.E. Martin, R.V. Marchetti, A.I. Cowan, S.M. Howitt, S. Broer, K. Kirk, Chloroquine transport *via* the malaria parasite's chloroquine resistance transporter, Science 325 (2009) 1680–1682.

[9] J.F. Trape, A. Tall, N. Diagne, O. Ndiath, A.B. Ly, J. Faye, F.D. Ba, C. Roucher, C. Bouganali, A. Badiane, F.D. Sarr, C. Mazenot, T. Balde, A.D. Raoult, P. Druilhe, O.M. Puijalon, C. Rogier, C. Sokhna, Malaria morbidity and pyrethroid resistance after the introduction of insecticide-treated bednets and artemisinin-based combination therapies: a longitudinal study, Lancet Infect. Dis. 11 (2011) 925–932.

[10] F. Cosledan, L. Fraisse, A. Pellet, F. Guillou, B. Mordmuller, P.G. Kremsner, A. Moreno, D. Mazier, J.–P. Maffrand, B. Meunier, Selection of a trioxaquine as an antimalarial drug candidate, Proc. Natl. Acad. Sci. 105 (2008) 17579–17584.

[11] (a) K. Singh, K. Singh, B. Wan, S. Franzblau, K. Chibale, J. Balzarini, Facile transformation of biginelli pyrimidin-2(1H)-ones to pyrimidines. In vitro evaluation as inhibitors of mycobacterium tuberculosis and modulators of cytostatic activity, Eur. J. Med. Chem. 46 (2011) 2290–2294;
(b) M.B. Deshmukh, S.M. Salunkhe, D.R. Patil, P.V. Anbhule, A novel and efficient one step synthesis of 2-amino-5-cyano-6-hydroxy-4-aryl pyrimidines and their anti-bacterial activity, Eur. J. Med. Chem. 44 (2009) 2651–2654;
(c) S. Rostamizadeh, M. Nojavan, R. Aryan, H. Sadeghian, M. Davoodnejad, A novel and efficient synthesis of pyrazolo [3, 4] pyrimidine derivatives and the study of their anti-bacterial activity, Chin. Chem. Lett. 24 (2013) 629–632;
(d) N.S. Habib, R. Soliman, K. Ismail, A.M. Hassan, M.T. Sarg, Pyrimidines. Part II: synthesis of novel pyrimidines, 1,2,4-triazolo[4,3-a]pyrimidin-7-ones and pyrimidino[2,1-c][1,2,4]triazin-8-ones for their antimicrobial and anticancer activities, Boll. Chim. Farm. 142 (2003) 396–405;
(e) T.G. Kvaljevic, M. Klika, M. Kvalj, I.M. Kleimer, S. Jurmanovic, A. Milic, J. Padovan, S. Raic-Malic, Synthesis, cytostatic activity and ADME properties of C-5 substituted and N-acyclic pyrimidine derivatives, Bioorg. Med. Chem. Lett. 22 (2012) 308–312;
(f) M.M. Mahmoud Ramiz, Wael, E. Sayed, E. Hagag, A.-H. Adel A. -Rahman, Synthesis and antiviral activity of new substituted pyrimidine glycosides, J. Hetrocycl. Chem. 48 (2011) 1028–1038;
(g) L.J. Liu, J.H. Hong, Synthesis and anti-Hiv activity of 4′-modified cyclopentenyl pyrimidine *c*-nucleosides, Nucleos. Nucleot. Nucl. 28 (2009) 303–314;
(h) M.S. Palanki, P.E. Erdman, L.M. Gayo-Fung, G.I. Shevlin, R.W. Sullivan, M.E. Goldman, L.J. Ransone, B.L. Bennett, A.M. Manning, M.J. Suto, Inhibitors of NF-κB and AP-1 gene expression: SAR Studies on the pyrimidine portion of 2-chloro-4-trifluoromethylpyrimidine-5-[*N*-(3′,5′-bis(trifluoromethyl)phenyl) carboxamide], J. Med. Chem. 43 (2000) 3995–4004;
(i) A. Agarwal, K. Srivastava, S.K. Puri, P.M.S. Chauhan, Synthesis of 2,4,6-trisubstituted pyrimidines as antimalarial agents, Bioorg. Med. Chem. 13 (2005) 4645–4650;
(j) H. Shao, S. Shi, S. Huang, A.J. Hole, A.Y. Abbas, S. Baumli, X. Liu, F. Lam, D.W. Foley, P.M. Fischer, M. Noble, J.A. Endicott, C. Pepper, S. Wang, Substituted 4-(thiazol-5-yl)-2-(phenylamino)pyrimidines are highly active cdk9 inhibitors: synthesis, x-ray crystal structures, structure–activity relationship, and anticancer activities, J. Med. Chem. 56 (2013) 640–659.

[12] (a) R. Oliveira, A.S. Newton, R.C. Guedes, D. Miranda, R.K. Amewu, A. Srivastava, J. Gut, P.J. Rosenthal, P.M. O'Neill, S.A. Ward, F. Lopes, R.A. Moreira, An endoperoxide-based hybrid approach to deliver falcipain inhibitors inside malaria parasites, Chem. Med. Chem. 8 (2013) 1528–1536;
(b) J.M. Coteron, D. Catterick, J. Castro, M.J. Chaparro, B. Díaz, E. Fernández, S. Ferrer, F.J. Gamo, M. Gordo, J. Gut, L. de Las Heras, J. Legac, M. Marco, J. Miguel, V. Muñoz, E. Porras, J.C. de La Rosa, J.R. Ruiz, E. Sandoval, P. Ventosa, P.J. Rosenthal, J.M. Fiandor, Falcipain inhibitors: optimization studies of the 2-pyrimidine carbonitrile lead series, J. Med. Chem. 53 (2010) 6129–6152.

[13] E. Altmann, S.W.C. Jacob, M. Missbach, Novel purine nitrile derived inhibitors of the cysteine protease cathepsin K, J. Med. Chem. 47 (2004) 5833–5836.

[14] (a) V. Ehmke, F. Kilchmann, C. Heindl, K. Cui, J. Huang, T. Schirmeister, F. Diederich, Peptidomimetic nitriles as selective inhibitors for the malarial cysteine protease falcipain-2, Med. Chem. Comm. 2 (2011) 800–804;
(b) V. Ehmke, J.E.Q. Quinsaat, P. Rivera-Fuentes, C. Heindl, C. Freymond, M. Rottmann, R. Brun, T. Schirmeister, F. Diederich, Tuning and predicting biological affinity: aryl nitriles as cysteine protease inhibitors, Org. Biomol. Chem. 10 (2012) 5764–5768.

[15] (a) R. Oliveira, R.C. Guedes, P. Meireles, I.S. Albuquerque, L.M. Goncalves, E. Pires, M.R. Bronze, J. Gut, P.J. Rosenthal, M. Prudencio, R. Moreira, P.M. O'Neill, F. Lopes, Tetraoxane-pyrimidine nitrile hybrids as dual stage antimalarials, J. Med. Chem. 57 (2014) 4916–4923.

[16] (a) K. Singh, H. Kaur, K. Chibale, J. Balzarini, S. Little, P.V. Bharatam, 2-Aminopyrimidine based 4-aminoquinoline anti-plasmodial agents. Synthesis, biological activity, structure-activity relationship and mode of action studies, Eur. J. Med. Chem. 52 (2012) 82–97;
(b) K. Singh, H. Kaur, K. Chibale, J. Balzarini, Synthesis of 4-aminoquinoline–pyrimidine hybrids as potent antimalarials and their mode of action studies, Eur. J. Med. Chem. 66 (2013) 314–323;
(c) K. Singh, H. Kaur, P. Smith, C. de Kock, K. Chibale, J. Balzarini, Quinoline–pyrimidine hybrids: synthesis, antiplasmodial activity, SAR and mode of action studies, J. Med. Chem. 57 (2014) 435–448.

[17] (a) S. Moore, H. Jaeschke, G. Kleinau, S. Neumann, S. Costanzi, J. Jiang, J. Childress, B.M. Raaka, A. Colson, R. Paschke, G. Krause, C.J. Thomas, M.C. Gershengorn, Evaluation of small-molecule modulators of the luteinizing hormone/choriogonadotropin and thyroid stimulating hormone receptors: structure–activity relationships and selective binding patterns, J. Med. Chem. 49 (2006) 3888–3896;
(b) C.O. Kappe, Recent advances in the biginelli dihydropyrimidine synthesis. New tricks from an old dog, Acc. Chem. Res. 33 (2000) 879–888.

[18] C.C. Musonda, S. Little, V. Yardley, K. Chibale, Application of multicomponent reactions to antimalarial drug discovery. Part 3: discovery of aminooxazole4-aminoquinolines with potent antiplasmodial activity in vitro, Bioorg. Med. Chem. Lett. 17 (2007) 4733–4736.

[19] P.B. Madrid, A.P. Liou, J.L.D. Risi, R.K. Guy, Incorporation of an intramolecular hydrogen-bonding motif in the side chain of 4-aminoquinolines enhances activity against drug-resistant *P. falciparum*, J. Med. Chem. 49 (2006) 4535–4543.

[20] T. Efferth, M.R. Romero, D.G. Wolf, T. Stamminger, J.J.G. Marin, M. Marschall, The antiviral activities of artemisinin and artesunate, Clin. Infect. Dis. 47 (2008) 804–811.

[21] E.E. Ooi, J.S.W. Chew, J.P. Loh, R.C.S. Chua, In vitro inhibition of human influenza A virus replication by chloroquine, Virol. J. 3 (2006) 39–41.

[22] A. Savirno, J.R. Boelaert, A. Cassone, G. Majori, R. Cauda, Effects of chloroquine on viral infections: an old drug against today's diseases? Lancet Infect. Dis. 3 (2003) 722–727.

[23] (a) A. Dorn, S.R. Vippagunta, H. Matile, C. Jaquet, J.L. Vennerstrom, R.G. Ridley, An assessment of drug-haematin binding as a mechanism for inhibition of haematin polymerisation by quinoline antimalarials, Biochem. Pharmacol. 55 (1998) 727–736;
(b) T.J. Egan, Interactions of quinoline antimalarials with hematin in solution, J. Inorg. Biochem. 100 (2006) 916–926.

[24] P. Gans, A. Sabatini, A. Vacca, Investigation of equilibria in solution. Determination of equilibrium constants with the hyperquad suite of programmes, Talanta 43 (1996) 1739–1753.

[25] W. Trager, J.B. Jensen, Human malaria parasite in continuous culture, Science 193 (1976) 673–675.

[26] M.T. Makler, J.M. Ries, J.A. Williams, J.E. Bancroft, R.C. Piper, B.L. Gibbins, D.J. Hinrichs, Parasite lactate dehydrogenase as an assay for *Plasmodium falciparum* drug sensitivity, Am. J. Trop. Med. Hyg. 48 (1993) 739–741.